MELT MIXED NANOCOMPOSITES OF PA12 WITH MWNT: INFLUENCE OF MWNT AND MATRIX PROPERTIES ON MACRODISPERSION AND ELECTRICAL PROPERTIES

*Robert Socher, Beate Krause, Regine Boldt, Petra Pötschke**
Leibniz Institute of Polymer Research Dresden, Hohe Strasse 6, 01069 Dresden, Germany
Sylvia Hermasch, Roland Wursche, Evonik Degussa GmbH, Paul-Baumann-Str. 1 45772 Marl, Germany

Abstract

Nanocomposites containing four different polyamide 12 (PA12) and three multiwalled carbon nanotubes (MWNTs) were prepared via small scale melt processing to study the effect of different MWNTs and the influence of polymer properties on the dispersion of the fillers and the electrical properties of the composites. Under the selected mixing conditions the lowest electrical percolation threshold of 0.7 wt% was found for Nanocyl^{TM} NC7000 in low viscous PA12. Moreover, big influences of the end group functionality (acid or amine excess) and the melt viscosity of the matrix were found. Composites of PA12 with acid excess showed lower percolation thresholds than those based on amino-terminated materials. At constant end group ratio low viscous matrices resulted in lower percolation thresholds than high viscous materials. The best MWNT dispersion was obtained in both high viscous PA12 composites. In these systems the mixing speed was varied indicating an optimum concerning electrical conductivity at 150 rpm as compared to 50 and 250 rpm.

Keywords: A. Carbon nanotubes, Nano composites, Polymer-matrix composites (PMCs); B. Electrical properties; D. Optical microscopy, Dispersion

* Corresponding author. Tel.: +49/3514658395; fax: +49/3514658565.
E-mail address: poe@ipfdd.de (P. Pötschke)

1. Introduction

With the implementation of a 200 tons/year plant for Baytubes® [1] and the coming start up in July 2010 of a 400 tons/year plant for Nanocyl™ NC 7000 [2], the carbon nanotube (CNT) producers are on their way to the world scale production of CNTs. In consequence, prices will drop and more and more potential applications [3-7] using the outstanding properties of CNTs like high mechanical strength [8] and electrical conductivity [8, 9] can enter the market.

An enormous increase in number of studies in the field of CNT nanocomposites could be observed over the last years [10-12], but still some problems like the incomplete dispersion and distribution of primary CNT agglomerates or the insufficient adhesion between CNTs and the polymer matrix in nanocomposites have to be solved.

For composites of polyamide 12 (PA12) containing CNTs potential application areas are e.g. antistatic fuel pipes and parts in fuel pumps for the use in the automotive industry. Due to economic reasons a low electrical percolation threshold is desired. The morphology of conductive fillers, like shape (spherical, rodlike, platelike, clustered) and the resulting aspect ratio, strongly influences their percolation threshold [13-15] in composites and thus for different kinds of fillers different electrical percolation threshold are observed [16]. Due to their very high aspect ratios CNTs are favourable for achieving low percolation thresholds. For bulk applications, most commercially available CNT represent multiwalled carbon nanotubes (MWNTs) produced by chemical vapour deposition where highly entangled MWNT agglomerates are formed. For the dispersion and distribution of nanotubes in polymer matrixes different techniques like solution mixing, in situ-polymerisation, the latex-approach, and melt mixing are applied. High mixing efficiency, working without solvents and short processing times make melt mixing the method of choice for industrial production of CNT composites. Hereby the dispersion of the nanotube agglomerates is influenced by many processing parameters like mixing speed, melt temperature, throughput or residence time [17-21]. Little attention has been paid to identify differences in the dispersion and electrical properties of different MWNT materials or the influence of polymer properties in melt mixed nanocomposites [22-28].

Most of the studies in literature concerning composites of polyamide and MWNTs are dealing with polyamide 6 (PA6) [18, 29-31] or polyamide 6.6 (PA66) [18]. For PA66 a percolation threshold of 1 wt% was reported, whereas those reported for PA6 appeared

to be higher starting at about 2.5 wt% for pressed plates when using Nanocyl^{TM} NC7000 in small scale melt mixing. For specially synthesized straight MWNTs having a low oxygen content on the surface and a high aspect ratio an ultralow percolation of 0.04 wt% could be observed in melt mixed PA6.6 composites as measured on pressed plates [22]. For PA6, Kodgire et al. [32] reported an electrical percolation threshold of only 0.5 wt% for MWNTs (Nanocyl, purity >95%, L/D= 10-1000) modified with sodium salt of 6-amoinohexanoic acid (Na-AHA). In contrast, nonmodified MWNTs showed a threshold between 2 – 3 wt% when using small-scale melt mixing and pressed plates. For PA12, only selected papers dealing with dispersion and/or electrical conductivity could be found. Ha et al. [33] found resistivity values lower than 10^7 Ohm-cm on pressed plates starting at 3 wt% MWNTs (Nanocyl^{TM} NC7000) addition in PA12 (Vestamid L1600 nf). The same value was reported by Bhattacharyya et al. [34, 35] for nonmodified single-walled carbon nanotubes (SWNTs, Nanoledge) when using a PA12 with equivalence of acid and amine end groups and a MFI of 154g/10 min (275°C, 5kg). After encapsulating the nanotubes using styrene-maleic-anhydride in order to create a reactive coupling to the matrix much better dispersion was found, however the composites were non conductive due to a bonded polymer layer around the nanotubes. As other polyamides, PA12 can be synthesized with different ratios of the end groups, namely amine or acid, which influence different properties, like mechanical. The selection of the end group ratio depends on the application and the additives in formulations; however, most of the industrial types are acid group terminated. In literature, most of the papers do not name the end group ratio. Thus, a comparison of different results may be difficult, if the end group termination plays a role on dispersion and conductivity. To our knowledge, no comparative study exists concerning dispersion and electrical properties of composites based on different end group terminated PA12. In this work, composites of different PA12 with diverse commercially available MWNTs were investigated to study the effect of the nanotube material as well as polymer matrix properties (especially end group functionalities and viscosity) on nanotubes macrodispersion and electrical properties. For these purpose PA12 types with preferential functionalities in two viscosity levels were used.

2. Experimental

2.1 Materials

Four different types of PA12 were supplied by Evonik Degussa GmbH (Marl, Germany). Among these types were two acid groups terminated and two amine group terminated PA12 with low or high viscosity. The materials are summarized in Table 1, showing also the end group contents as obtained by titration and melt viscosities at processing temperatures as studied using an ARES oscillatory rheometer (Rheometric Scientific Inc., Piscataway, NJ, USA) with parallel plate geometry in nitrogen atmosphere.

The following multiwalled carbon nanotubes (MWNT) were employed: Baytubes® C150P (Bayer MaterialScience AG, Leverkusen, Germany), Nanocyl™ NC7000 (Nanocyl S.A., Sambreville, Belgium), and FutureCarbon CNT-MW-K (FutureCarbon GmbH, Bayreuth, Germany). For comparison, Printex® XE2 (Evonik Degussa GmbH, Marl, Germany) was used as Carbon Black (CB). This CB has a BET-surface area of 910 m^2/g [36]. The properties of the MWNT materials and CB as given in the corresponding data sheets are shown in Table 2.

Octadecylamine (purity > 90%) was supplied by Fluka (Fluka Chemie GmbH, Buchs, Switzerland) and was used without further purifications.

2.2 Processing

Melt mixing of the granular polymer (dried overnight at 80°C) and the powdery MWNT (dried overnight at 120°C) was done in a DACA microcompounder (DACA Instruments, Santa Barbara, USA; inner volume: 4.5 ccm). Polymer and CNTs were alternatively added to the microcompounder (at least 3 portions). Melt mixing was performed at 210°C with a mixing speed of 250 rpm for 5 min (low viscous PA12). In high viscous systems, a mixing temperature of 260°C was used to enable processability. The relatively high mixing speed was selected as in [17, 18] better dispersion was achieved at higher mixing speed; the mixing time was set considering the maximum mixing time achievable in industrial twin-screw extrusion. These mixing conditions do not represent optimized condition which may be different for diverse nanotube materials.

For some experiments, octadecylamine was used to prevent a cross-linking of PA12 and utilised in excess to the amine groups of the PA12. It was dispensed in the microcompounder at the end of the filling process.

The extruded strands were cut into pieces of some millimetres and compression moulded into plates (30 mm diameter, 0.5 mm thickness) using a Weber hot press

(Model PW 40 EH, Paul Otto Weber GmbH, Remshalden, Germany). Compression moulding was performed following the procedure given in [17] with a pressing temperature of 220°C for low viscous PA12 composites, and 260°C for high viscous PA12. The pressing speed was 6 mm/min with a pressing time of 1 min and the pressing force was increased in steps up to 100 kN.

2.3 Characterization

The electrical volume resistivity was measured using a Keithley Electrometer 6517A (Keithley Instruments Inc., Cleveland, USA) combined with an 8009 Resistivity Test Fixture for samples with a volume resistivity > 10^7 Ohm cm (unfilled symbols in the graphs). An intermediate isolation film (thickness < 0.5 mm) with a hole of 30 mm in diameter was used to reduce the measuring area of the Test Fixture and the measured values were corrected accordingly. For volume resistivity values lower than 10^7 Ohm cm (filled symbols in the graphs), a 4-point test fixture (gold contact wires with a distance of 16 mm between the source electrodes and 10 mm between the measuring electrodes) combined with the Keithley Electrometer 6517A was applied on strips (30 x 3 x 0.5 mm^3) cut from the pressed plates. For discussion, resistivity values were converted into electrical conductivity values. At least four values were measured for each sample and the standard deviation is given as error bars in the figures.
If possible, the electrical percolation thresholds (p_c) were fitted using the power law function for the composite conductivity near the electrical percolation threshold [37]:

$$\sigma(p) = B(p - p_c)^t \qquad (1)$$

with the experimental conductivity value $\sigma(p)$ for concentrations $p > p_c$, the proportionality constant B, the electrical percolation threshold p_c and the critical exponent t, using the method of mean square error minimisation.
The state of CNT macrodispersion in the composites was studied using light transmission microscopy analysing remaining primary agglomerates with sizes > 5 µm. Thin sections of 5 µm thickness were prepared in perpendicular direction to the extruded strands using a Leica RM 2155 microtome (Leica Microsystems GmbH, Wetzlar, Germany). The samples were characterized with a microscope BH2 in transmission mode combined with a camera DP71 (Olympus Deutschland GmbH, Hamburg, Germany). The ratio A/A_0 was determined from the light micrographs by calculating the ratio of the area A of remaining agglomerates to the total area of the micrograph A_0 (~ 0.6 mm^2) using the software ImageJ Version 1.43g. For

quantification, at least 7 cuts were investigated for each sample, and the standard deviation between the seven cuts is mentioned. In addition, the number of agglomerates per mm^2 was evaluated.

Scanning electron microscopy (SEM) was performed on the as delivered CNT materials and selected composites using an Ultra Plus Field Emission Gun Scanning Electron Microscope (FEG-SEM, Carl–Zeiss AG, Oberkochen, Germany). Surfaces of pressed plates of the composites were analysed using the charge contrast imaging (CCI) mode using an InLens-detector which clearly shows the electrical conductive filler network of the sample. The neat CNT materials were discarded on a double-sided adhesive copper tape and monitored using a SE2-Detector.

3. Results and discussion

3.1 The influence of CNT material

SEM images of the different pristine MWNT powders are shown in Figure 1. For FutureCarbon CNT-MW-K and Baytubes® C150P a bird nest structure was found, whereas a combed yarn structure was observed for Nanocyl™ NC7000. Especially the agglomerate structure of the Baytubes® C150P appears to be very compact. When comparing the dispersability of different nanotubes in aqueous surfactant solutions, Krause et al. [38] reported a worse behaviour and higher agglomerates strength for Baytubes® C150 in comparison to Nanocyl™ NC7000 and FutureCarbon CNT-MW-K which may be also related to the much higher bulk density (see Table 2) and the resulting higher packing density within the primary agglomerates.

The effect of the nanotube materials was investigated using low viscous PA12 with acid group excess. Figure 2 shows the electrical percolation behaviour for the three carbon nanotubes and carbon black, in which the lines represent the percolation curves fitted according to equation (1). Electrical percolation was found at lower filler contents for the investigated MWNT in comparison to the CB due to their higher aspect ratio. In addition, huge differences were found in the electrical percolation thresholds of the investigated CNTS which varied between 0.7 wt% for Nanocyl™ NC7000, 1.3 wt% for FutureCarbon CNT-MW-K, and 2.1 wt% for Baytubes® C150P. The electrical percolation threshold of PA12 composites containing Printex® XE2 was determined at a filler content of 4.3 wt%. The highest electrical conductivity value at loadings of 5 wt% filler was found for Nanocyl™ NC7000.

The macrodispersion of the remaining MWNT agglomerates was investigated for composites containing 2 wt% filler and is shown exemplarily in light micrographs in Figure 3. The lowest area ratio A/A_0 of remaining agglomerates was found with 0.3 % ± 0.1 for the FutureCarbon CNT-MW-K. In addition this sample showed only 17 particles/mm^2. In case of Nanocyl^{TM} NC7000, the average area ratio of the remaining agglomerates was measured to be 1.3 % ± 0.6 and 24 particles/mm^2 were found. The agglomerates showed a broad agglomerate size distribution. For Baytubes® C150P samples, the area ratio of remaining agglomerates was 1.3% ± 0.4. This sample indicated the biggest remaining agglomerates of all investigated ones with sizes up to nearly 100 µm and with 31 particles/mm^2 the highest number of agglomerates.
The results indicate the best state of macrodispersion among the MWNT investigated for FutureCarbon CNT-MW-K. Obviously the nanotube materials show different dispersability in the melt as it was shown previously for their dispersability in aqueous surfactant dispersions and can be assigned to the different agglomerate structure as discussed before. It may be assumed that the melt infiltration process of polymer chains into agglomerates leading to reduced agglomerate strength is more difficult in the case of Baytubes® C150 as compared to the more loosely packed agglomerates of Nanocyl^{TM} NC7000 and FutureCarbon CNT-MW-K.
However, although in the case of FutureCarbon CNT the dispersion of primary agglomerates was quite good these composites did not show the lowest electrical percolation threshold. Generally, at low amount of remaining primary agglomerates more individualized nanotubes are available for the formation of the conductive network. However, the results indicate that not only the state of macrodispersion is responsible for high electrical conductivity, but also dispersion and nanotube arrangement in micro- and nanoscale not assessed by light microscopy. In addition, different length of the initial and possibly shortened nanotubes after processing may lead to different aspect ratios which also influence both; the dispersability and the electrical percolation threshold. Hereby thicker and shorter nanotubes can be dispersed more easily [25, 39] but result on the other hand in higher percolation thresholds.
To visualize the dispersion structure and conductive network of nanotubes in the composites containing 2 wt% MWNT, the samples were analysed by charge contrast imaging (Figure 4). In this mode only those CNTs near the surface can be seen which are part of a conductive network. The SEM-CCI images of NC7000 (Fig. 4A) indicate that a homogeneous distribution of nanotubes in the composite was achieved which

leads to the formation of many percolation pathways in the matrix. This finding is in accordance with the electrical conductivity values of 3.4 E-5 S/cm for the 2 wt% NC7000 sample which is the highest for the investigated MWNT materials. In samples containing 2 wt% FutureCarbon MW-K (Fig. 4B) a cluster percolation of MWNT agglomerates can be observed. Here, the MWNT form small agglomerates in the size range of a few micrometers that are quite uniformly dispersed in the matrix which led to lower conductivity values than for the NC7000 sample. For the nonconductive composite containing 2 wt% Baytubes, the formation of a percolation network was not detected. On selected locations, only some CNT agglomerates can be seen on the surface of the pressed sample (Fig. 4C).

In comparison to the CNT composites those with CB Printex® XE2 exhibited the best macrodispersion as observed by light microscopy. The A/A_0 index was measured to be 0.2 % and only very few particles larger than 15 µm (0.2 particles/mm^2) were observed. Whereas CNTs tend to form entangled agglomerates based on high van der Waals forces, CB agglomerate structures seem to need much lower shear forces to their dispersion and distribution in the polymer melt. On the other hand, because of their more spherical morphology, much higher filler content is needed to form an electrically conductive network as it was observed in the experiments.

3.2 The influence of matrix properties

For the investigation of the influence of matrix properties like viscosity and end group functionalisation on the electrical percolation behaviour and the state of the dispersion in the matrix, PA12 composites containing Baytubes® C150P were chosen. Firstly, the complex viscosity was measured for the four neat types of PA12 at the respective processing temperatures (Figure 5, see Table 1). The low viscous PA12 types showed at 210°C nearly frequency independent complex viscosity values of 150 Pa s (acid excess) and 115 Pa s (amine excess). The complex viscosity measured at 260°C and 0.1 rad/s for high viscous PA12 with amine excess (14,950 Pa s) was higher than for the PA12 with acid excess (5,630 Pa s). However, in the high frequency range (100 rad/s) comparable viscosity levels for acid and amine group terminated PA12 at the processing temperatures were found.

The electrical percolation behaviour of the different samples is shown in Figure 6. The lowest electrical percolation threshold was observed with 2.1 wt% for the composites with low viscous PA12 and acid group termination. The composites with amine excess

and low viscosity showed a significantly higher electrical percolation threshold of 3.7 wt%. This implies a big influence of the end group termination in low viscous PA12 composites regarding to the electrical percolation behaviour.

An influence of the end group termination was also observed for the high viscous system. The percolation threshold was found at 3.6 wt% for acid excess, whereas for amine excess no clear percolation transition could be found. Enhanced conductivity is reached at 4 wt%. However, the addition of higher CNT amounts was not possible due to torque limitation of the DACA microcompounder in the investigated concentration range.

The influences of the end group functionality and the viscosity of the matrix in PA12 composites containing 2 wt% Baytubes® C150P on the macrodispersion is shown in the micrographs of Figure 7. The highest area ratio of remaining agglomerates was found with 2.5 % ± 0.9 for the low viscous amino-terminated PA12 composites. For this type the highest number of particles (69 particles/mm^2) and large particle sizes up to 85 µm were observed. Somewhat better dispersion was observed using low viscous acid-terminated PA12 with an area ratio of remaining agglomerates of 1.3% ± 0.4 and 31 particles/mm^2. The best dispersion was obtained for the composites based on high viscous PA12 matrices, even if here the electrical percolation thresholds were the highest. Here, no differences in the amount of remaining agglomerates between samples containing PA12 with acid or amine excess were found: the A/A_0 ratio was only 0.3% ± 0.2 and no remaining agglomerates larger than 50 µm were observed in the samples. In case of acid terminated PA12 composites 15 particles/mm^2 were found and 22 particles/mm^2 were observed for amine excess whereas these particles were very small.

When comparing the composites based on low and high viscous PA12 matrix, the torque values and consequently the shear forces during melt mixing of the high viscous PA12 types were much higher, even if the melt temperature were selected differently. Next to better dispersion especially due to the agglomerate rupture process [40] this could promote damaging or shortening of the nanotubes during the processing which inevitably leads to a decrease of the aspect ratio [41, 42]. A decline of the aspect ratio could be a reason for the rather high electrical percolation thresholds in the composites based on high viscous PA12.

Comparing the effects of acid and amine termination, big differences in dispersion and electrical percolation were observed despite comparable PA12 melt viscosities and

applied shear forces. Interestingly, during mixing of both amine terminated matrices an increase in torque was observed as well without as with nanotubes. This indicates changes in the polymer structure during mixing which may be assigned to a shear stress induced cross-linking as discussed in [18] for PA6. By a reaction of two amino end groups, a secondary amine can be formed under elimination of ammonia. The secondary amine is able to react with an acid end group of a PA12 chain, which could lead to a branching at the *N,N'*-disubstituted amide group. This behaviour has already been described for PA6.6 [43]. This assumption could explain the hindering of nanotube network formation in amine excess composites. In addition, a certain extent of reaction of the amine end groups with oxygen functionalities present on the surface of Baytubes C150P [44] (or nondispersed agglomerates) may not be excluded which would not happen in that extent in case of acid terminated nanotubes.

A possible way to reduce the branching of the PA12 chains is to promote the faster reaction of an amine (here of octadecylamine) with a PA12 amine end group, which reduces the chances for the reaction of two PA12 amine end groups. For this purpose, octadecylamine was added to the low viscous amine terminated PA12 and MWNT at the end of the filling process into the microcompounder. By that, the increase of torque during melt mixing was nearly completely suppressed. Therefore, it can be concluded that the assumed reaction of two PA12 chains terminated with amine groups and the following cross-linking could be significantly reduced. Adding octadecylamine to low viscous PA12 with 2 wt% Baytubes® C150P resulted in better macrodispersion as indicated by a decrease in A/A_0.from 2.4 % ± 0.9 (69 particles/mm^2) without octadecylamine to 1.4 % ± 0.5 (37 particles/mm^2). This result is quite similar to the value of 1.3 % ± 0.4 for composites based on low viscous PA12 with acid excess, where cross-linking during melt mixing was not observed.

3.3 The influence of mixing speed

Although the dispersion in high viscous PA12 composites containing Baytubes® C150P was quite good and only small remaining agglomerates were found, the electrical percolation thresholds were very high. As it was described by different authors that the processing conditions in small-scale melt mixing can influence the electrical percolation threshold [17, 18], for high viscous PA12 variations in the mixing speeds were performed (Figure 8). Next to the already investigated mixing speed of 250 rpm also lower mixing speeds (50 rpm, 150 rpm) were applied. For amine as well as acid group

terminated high viscous PA12 composites containing Baytubes® the highest conductivity values at MWNT contents of 3 and 4 wt% were found using a mixing speed of 150 rpm (see Figure 10A and B). As compared to 250 rpm at lower mixing speeds percolation is shifted to lower values in case of acid terminated PA12. Whereas at 250 rpm the percolation threshold was fitted to be at 3.7 wt%, percolation is already achieved at 3 wt% when using 50 or 150 rpm. For amine terminated PA12 no such clear percolation curves could be obtained as due to the torque limit of the mixer the highest possible filling level was 5 wt% which is still within the percolation range (see Figure 10B). However, at 4 and 5 wt% MWNT loading mixing at 50 rpm led to the lowest conductivity values, whereas for 150 and 250 rpm percolation is already reached at 4 wt%.

The results indicate an optimum of mixing speed at 150 rpm concerning the electrical percolation threshold. It seems that at the low speed of 50 rpm the macrodispersion is worse as bigger and more numerous agglomerates leading to a higher area ratio were found for both high viscous PA12 (results for acid excess see Figure 9). At the high speed of 250 rpm the macrodispersion is quite good, however due to the much higher shear forces a more pronounced breaking of nanotubes may be assumed, leading to a decrease in the effective aspect ratio.

Summary and Conclusion

In this study the influence of different MWNT materials as well as matrix properties of PA12 like end group termination and melt viscosity on the electrical percolation threshold and state of CNT dispersion in composites melt mixed in a small scale microcompounder were investigated.

The different investigated MWNTs showed huge differences considering their electrical percolation thresholds as analysed using low viscous PA12 with acid excess. For composites containing Nanocyl™ NC7000, the lowest electrical percolation threshold (0.7 wt%) was found as well as the highest conductivity value for high MWCNT contents (2.8E-03 S/cm at 5 wt%). As the morphological features like length, diameter and purity of the nanotubes were similar, it can be assumed that a more complete individualization of the primary agglomerates into single nanotubes in combination with a faster formation of a conductive network of these nanotubes was achieved in comparison to the Future Carbon MW-K-T and Baytubes® C150P nanotubes. As shown in SEM images, already the structure of the primary agglomerates of the starting

nanotube materials which had to be dispersed in the melt mixing process were quite different.

A significant influence of the PA12 end group functionality on the dispersion of CNTs and the electrical behaviour of the composites was observed as investigated using Baytubes® C150P. Here, the best dispersion and electrical properties (percolation threshold at 2.1 wt%) were found for composites based on PA12 with acid group termination in comparison to the other investigated types of PA12. For PA12 with amine group excess, the reaction between two of these groups and a following cross-linking under the formation of a *N,N'*-disubstituted amide group was supposed, which can hinder the nanotube dispersion and explains the high percolation threshold of 4.3 wt%. The results clearly indicate that the end group ratio has to be considered when discussing dispersion and electrical properties of PA12 based CNT composites. For achieving low electrical percolation, low viscous acid based formulations seem to be favourable.

Concerning the influence of mixing speed on electrical percolation, an optimum was found at 150 rpm as compared to 50 and 250 rpm as investigated on high viscous PA12 with Baytubes® C150P. For polyamide containing acid termination a clear lowering of percolation concentration by nearly 1 wt% was observed when comparing 150 rpm versus 250 rpm whereas for amine terminated PA12 higher conductivity values were obtained. This implies that a balance between achieving suitable dispersion and retaining the high aspect ratio of nanotubes is important for achieving low electrical percolation thresholds.

Acknowledgement

We thank the German Federal Ministry of Education (BMBF) for financial support within the Innovation Alliance Inno.CNT, project CarboDis, BMBF 03X0042M.

References

[1] Bayer MaterialScience opens world's largest carbon nanotube pilot facility. 2010 [cited 2010 20.02.2010]; 200t/year CNT Plant by Bayer]. Available from: http://www.baytubes.com/news_and_services/pr_100129_new_facility.html

[2] Nanocyl to Expand Global Production Capacity of Carbon Nanotubes. 2009 [cited 2010 20.02.2010]; Available from: http://www.nanocyl.com/en/News/Nanocyl-to-Expand-Global-Production-Capacity-of-Carbon-Nanotubes

[3] Baughman RH, Zakhidov AA, de Heer WA. Carbon nanotubes - the route toward applications. Science 2002;297(5582):787-792.

[4] Bandaru PR. Electrical properties and applications of carbon nanotube structures. Journal of Nanoscience and Nanotechnology 2007;7(4-5):1239-1267.
[5] Zhang CS, Ni QQ, Fu SY, Kurashiki K. Electromagnetic interference shielding effect of nanocomposites with carbon nanotube and shape memory polymer. Composites Science and Technology 2007;67(14):2973-2980.
[6] Bianco A, Kostarelos K, Partidos CD, Prato M. Biomedical applications of functionalised carbon nanotubes. Chemical Communications 2005;(5):571-577.
[7] Agui L, Yanez-Sedeno P, Pingarron JM. Role of carbon nanotubes in electroanalytical chemistry - A review. Analytica Chimica Acta 2008;622(1-2):11-47.
[8] Treacy MMJ, Ebbesen TW, Gibson JM. Exceptionally high Young's modulus observed for individual carbon nanotubes. Nature 1996;381(6584):678-680.
[9] Wei BQ, Vajtai R, Ajayan PM. Reliability and current carrying capacity of carbon nanotubes. Applied Physics Letters 2001;79(8):1172-1174.
[10] Bauhofer W, Kovacs JZ. A review and analysis of electrical percolation in carbon nanotube polymer composites. Composites Science and Technology 2009;69(10):1486-1498.
[11] McClory C, Chin SJ, McNally T. Polymer/Carbon Nanotube Composites. Australian Journal of Chemistry 2009;62(8):762-785.
[12] Spitalsky Z, Tasis D, Papagelis K, Galiotis C. Carbon nanotube-polymer composites: Chemistry, processing, mechanical and electrical properties. Progress in Polymer Science 35(3):357-401.
[13] Kirkpatrick S. Percolation and Conduction. Reviews of Modern Physics 1973;45(4):574-588.
[14] Balberg I, Anderson CH, Alexander S, Wagner N. Excluded Volume and its Relation to the Onset of Percolation. Physical Review B 1984;30(7):3933-3943.
[15] Li J, Ma PC, Chow WS, To CK, Tang BZ, Kim JK. Correlations between percolation threshold, dispersion state, and aspect ratio of carbon nanotubes. Advanced Functional Materials 2007;17(16):3207-3215.
[16] Pötschke P, Abdel-Goad M, Pegel S, Jehnichen D, Mark JE, Zhou DH, Heinrich G. Comparisons Among Electrical and Rheological Properties of Melt-Mixed Composites Containing Various Carbon Nanostructures. Journal of Macromolecular Science Part a-Pure and Applied Chemistry 47(1):12-19.
[17] Kasaliwal G, Göldel A, Pötschke P. Influence of processing conditions in small-scale melt mixing and compression molding on the resistivity and morphology of polycarbonate-MWNT composites. Journal of Applied Polymer Science 2009;112(6):3494-3509.
[18] Krause B, Pötschke P, Häußler L. Influence of small scale melt mixing conditions on electrical resistivity of carbon nanotube-polyamide composites. Composites Science and Technology 2009;69(10):1505-1515.
[19] Pujari S, Ramanathan T, Kasimatis K, Masuda J, Andrews R, Torkelson JM, Brinson LC, Burghardt WR. Preparation and Characterization of Multiwalled Carbon Nanotube Dispersions in Polypropylene: Melt Mixing Versus Solid-State Shear Pulverization. Journal of Polymer Science Part B-Polymer Physics 2009;47(14):1426-1436.
[20] Villmow T, Pötschke P, Pegel S, Häussler L, Kretzschmar B. Influence of twin-screw extrusion conditions on the dispersion of multi-walled carbon nanotubes in a poly(lactic acid) matrix. Polymer 2008;49(16):3500-3509.
[21] Villmow T, Kretzschmar B, Pötschke P. Influence of screw configuration, residence time, and specific mechanical energy in twin-screw extrusion of polycaprolactone/multi-walled carbon nanotube composites. Composites Science and Technology 2010; 70(14):2045–2055.

[22] Krause B, Ritschel M, Täschner C, Oswald S, Gruner W, Leonhardt A, Pötschke P. Comparison of nanotubes produced by fixed bed and aerosol-CVD methods and their electrical percolation behaviour in melt mixed polyamide 6.6 composites. Composites Science and Technology 2010;70(1):151-160.
[23] Pegel S, Pötschke P, Petzold G, Alig I, Dudkin SM, Lellinger D. Dispersion, agglomeration, and network formation of multiwalled carbon nanotubes in polycarbonate melts. Polymer 2008;49(4):974-984.
[24] Micusik M, Omastova M, Krupa I, Prokes J, Pissis P, Logakis E, Pandis C, Pötschke P, Pionteck J. A Comparative Study on the Electrical and Mechanical Behaviour of Multi-Walled Carbon Nanotube Composites Prepared by Diluting a Masterbatch With Various Types of Polypropylenes. Journal of Applied Polymer Science 2009;113(4):2536-2551.
[25] Morcom M, Atkinson K, Simon GP. The effect of carbon nanotube properties on the degree of dispersion and reinforcement of high density polyethylene. Polymer 2010;51(15):3540-3550.
[26] Krause B, Petzold G, Pegel S, Pötschke P. Correlation of carbon nanotube dispersability in aqueous surfactant solutions and polymers. Carbon 2009;47(3):602-612.
[27] Pötschke P, Fischer D, Simon F, Liane Hl, Magrez A, Forro L. Multiwalled Carbon Nanotubes Produced by a Continuous CVD Method and Their Use in Melt Mixed Composites with Polycarbonate. Macromolecular Symposia 2007;254:392-399.
[28] Pötschke P, Bhattacharyya AR, Janke A, Pegel S, Leonhardt A, Taschner C, Ritschel M, Roth S, Hornbostel B, Cech J. Melt mixing as method to disperse carbon nanotubes into thermoplastic polymers. Fullerenes Nanotubes and Carbon Nanostructures 2005;13:211-224.
[29] Logakis E, Pandis C, Peoglos V, Pissis P, Pionteck J, Pötschke P, Micusík M, Omastová M. Electrical/dielectric properties and conduction mechanism in melt processed polyamide/multi-walled carbon nanotubes composites. Polymer 2009;50(21):5103-5111.
[30] Saeed K, Park SY. Preparation of multiwalled carbon nanotube/nylon-6 nanocomposites by in situ polymerization. Journal of Applied Polymer Science 2007;106(6):3729-3735.
[31] Meincke O, Kaempfer D, Weickmann H, Friedrich C, Vathauer M, Warth H. Mechanical properties and electrical conductivity of carbon-nanotube filled polyamide-6 and its blends with acrylonitrile/butadiene/styrene. Polymer 2004;45(3):739-748.
[32] Kodgire PV, Bhattacharyya AR, Bose S, Gupta N, Kulkarni AR, Misra A. Control of multiwall carbon nanotubes dispersion in polyamide6 matrix: An assessment through electrical conductivity. Chemical Physics Letters 2006;432(4-6):480-485.
[33] Ha H, Ha K, Kim SC. An empirical equation for electrical resistivity of thermoplastic polymer/multi-walled carbon nanotube composites. Carbon 2010;48(7):1939-1944.
[34] Bhattacharyya AR, Pötschke P, Abdel-Goad M, Fischer D. Effect of encapsulated SWNT on the mechanical properties of melt mixed PA12/SWNT composites. Chemical Physics Letters 2004;392(1-3):28-33.
[35] Bhattacharyya AR, Bose S, Kulkarni AR, Pötschke P, Haussler L, Fischer D, Jehnichen D. Styrene maleic anhydride copolymer mediated dispersion of single wall carbon nanotubes in polyamide 12: Crystallization Behavior and morphology. Journal of Applied Polymer Science 2007;106(1):345-353.
[36] GmbH ED. Data sheet Printex(R) XE2, Edition 1.15/DE, 09.12.2008. 2008.
[37] Stauffer D, Aharony A. Introduction in percolation theory. London: Taylor and Francis, 1994.

[38] Krause B, Mende M, Pötschke P, Petzold G. Dispersability and particle size distribution of CNTs in an aqueous surfactant dispersion as a function of ultrasonic treatment time. Carbon 2010 accepted.
[39] Kasaliwal GR, Villmow T, Pegel S, Pötschke P. Influence of material and processing parameters on carbon nanotube dispersion in polymer melts: Woodhead Publishing Limited 2011.
[40] Kasaliwal GR, Pegel S, Göldel A, Pötschke P, Heinrich G. Analysis of agglomerate dispersion mechanisms of multiwalled carbon nanotubes during melt mixing in polycarbonate. Polymer 2010;51(12):2708-2720.
[41] Fu S-Y, Chen Z-K, Hong S, Han CC. The reduction of carbon nanotube (CNT) length during the manufacture of CNT/polymer composites and a method to simultaneously determine the resulting CNT and interfacial strengths. Carbon 2009;47(14):3192-3200.
[42] Andrews R, Jacques D, Minot M, Rantell T. Fabrication of carbon multiwall nanotube/polymer composites by shear mixing. Macromolecular Materials and Engineering 2002;287(6):395-403.
[43] Horbach A, Alewelt W, Müller H. Bestimmung von sekundären Aminogruppen als Fehlstrukturen in Polyamid-6.6. Makromol Chem 1985;186:2535-2538.
[44] Tessonnier JP, Rosenthal D, Hansen TW, Hess C, Schuster ME, Blume R, Girgsdies F, Pfander N, Timpe O, Su DS, Schlogl R. Analysis of the structure and chemical properties of some commercial carbon nanostructures. Carbon 2009;47(7):1779-1798.
[45] BayerMaterialScienceAG. Data sheet Baytubes® C150P. Edition 2006-01-18. 2006.
[46] Nanocyl. Data sheet Nanocyl 7000. Edition 2007-02-05. Sambreville, Belgium; 2007.
[47] FutureCarbon. Product Information Multiwalled Carbon Nanotubes (CNT-MW).

Tables:

Table 1 Characteristics of the PA12 types (end group contents and melt viscosity)

PA12 type	[COOH] content [mmol/kg]	[NH_2] content [mmol/kg]	Ieta*I at 100 rad/s [Pa-s (T_{melt})]
low viscous, acid excess	104	4.2	140 (210°C)
low viscous, amine excess	26	126	100 (210°C)
high viscous, acid excess	42	0.47	1240 (260°C)
high viscous, amine excess	3	56	1140 (260°C)

Table 2. Properties of the used CNT according to the supplier [45-47].

	Diameter [nm]	Length [µm]	Carbon purity [%]	Bulk density [kg/m^3]
Baytubes® C150P	13 - 16	1 - >10	> 95	120 – 170
Nanocyl™ NC7000	9.5 (average)	1.5 (average)	> 90	66*
FutureCarbon MW-K	15	-	90	28*
Printex® XE2	30 - 35	n. a.	> 99	100 - 400

* according to ref. [38]

Figure captions

Figure 1. Scanning electron microscopy images of pristine MWNT powder at two magnifications: (A) Nanocyl™ NC7000, (B) Baytubes® C150P, (C) FutureCarbon CNT-MW-K

Figure 2. Electrical volume conductivity of polyamide 12 composites containing different MWNT and CB

Figure 3. Light microscopy images of composites based on low viscous PA12 (acid excess) with 2 wt% filler content, A) Nanocyl™ NC7000, B) Future Carbon CNT-MW-K, C) Baytubes® C150 P, D) Printex® XE2

Figure 4. Scanning electron microscopy-charge contrast imaging micrographs of composites containing 2 wt% MWNT in low viscous PA12 with acid excess. A) Nanocyl™ NC7000, B) FutureCarbon CNT-MW-K, C) Baytubes® C150P

Figure 5. Complex melt viscosity |eta*| of different neat PA12 types in dependence on frequency at their processing temperatures

Figure 6. Electrical volume conductivity of different polyamide 12 composites containing Baytubes® C150P

Figure 7. Light microscopy images of PA12 containing 2 wt% Baytubes® C150P: A) low viscosity, acid excess, B) low viscosity, amine excess, C) high viscosity, acid excess, D) high viscosity, amine excess

Figure 8. Electrical volume conductivity of high viscous polyamide 12 composites containing Baytubes® C150P at different mixing speed: A) acid excess, B) amine excess

Figure 9. Light microscopy images of high viscous PA12 (acid excess) containing 2 wt% Baytubes® C150P prepared at different mixing speeds

A

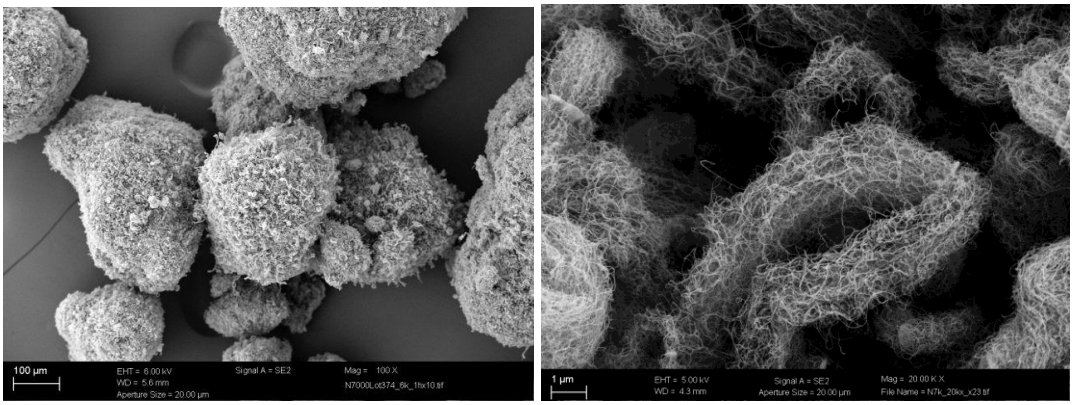
100 µm
EHT = 6.00 kV
WD = 5.6 mm
Aperture Size = 20.00 µm
Signal A = SE2
Mag = 100 X
N7000Lot374_6k_1hx10.tif
1 µm
EHT = 5.00 kV
WD = 4.3 mm
Signal A = SE2
Aperture Size = 20.00 µm
Mag = 20.00 K X
File Name = N7k_20kx_x23.tif

B

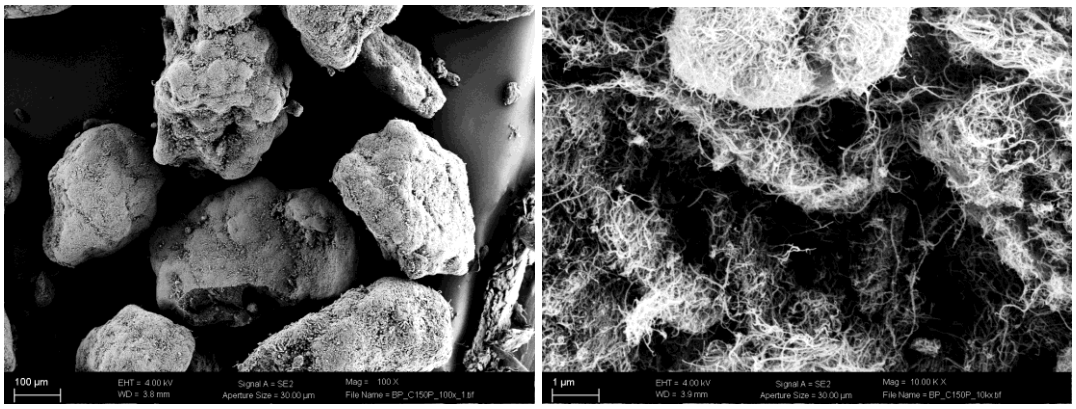
100 µm
EHT = 4.00 kV
WD = 3.8 mm
Signal A = SE2
Aperture Size = 30.00 µm
Mag = 100 X
File Name = BP_C150P_100x_1.tif
1 µm
EHT = 4.00 kV
WD = 3.9 mm
Signal A = SE2
Aperture Size = 30.00 µm
Mag = 10.00 K X
File Name = BP_C150P_10kx.tif

C

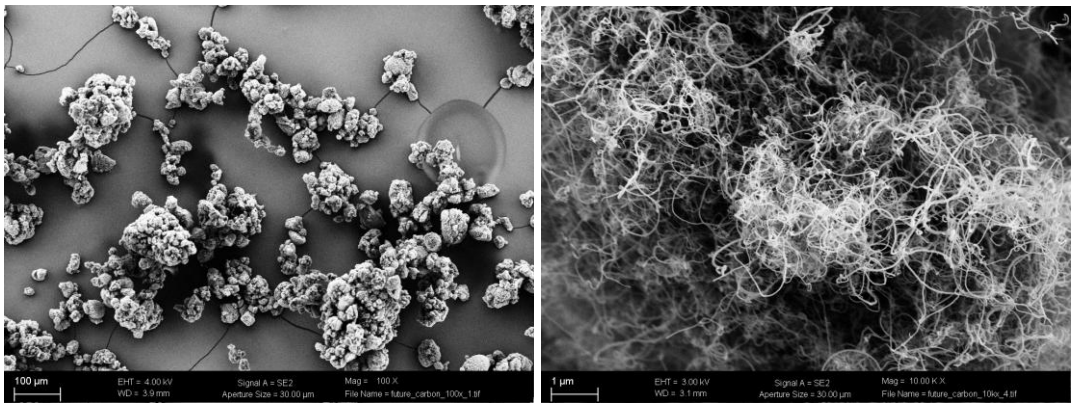
100 µm
EHT = 4.00 kV
WD = 3.9 mm
Signal A = SE2
Aperture Size = 30.00 µm
Mag = 100 X
File Name = future_carbon_100x_1.tif
1 µm
EHT = 3.00 kV
WD = 3.1 mm
Signal A = SE2
Aperture Size = 30.00 µm
Mag = 10.00 K X
File Name = future_carbon_10kx_4.tif

Figure 1

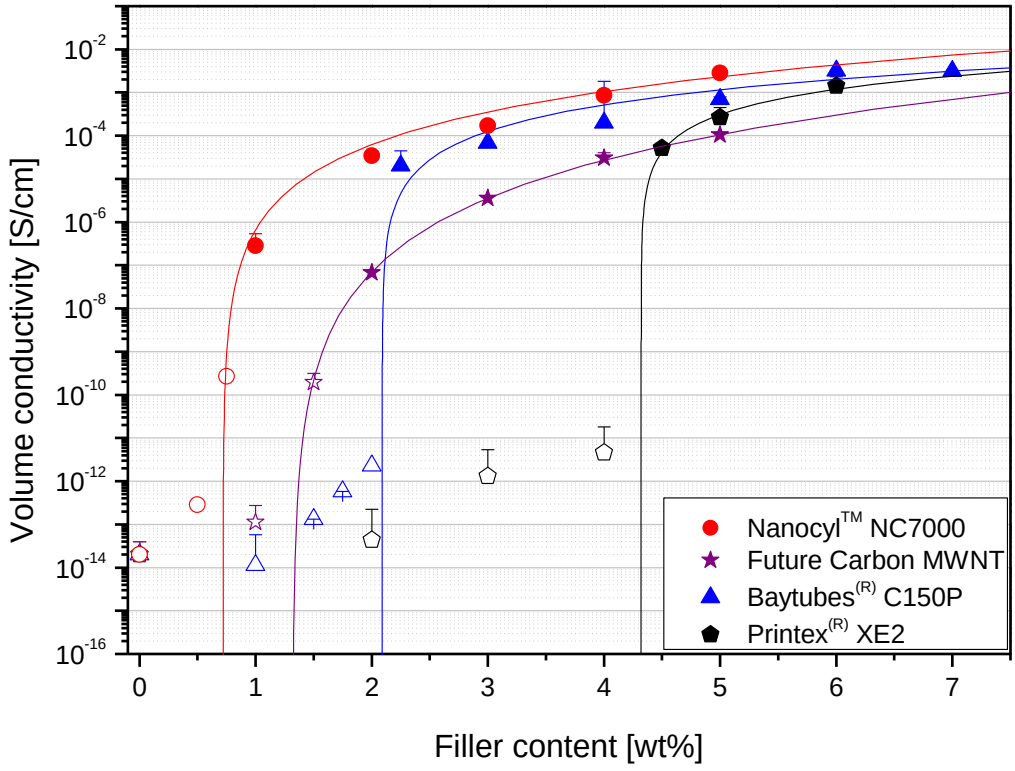

Figure 2

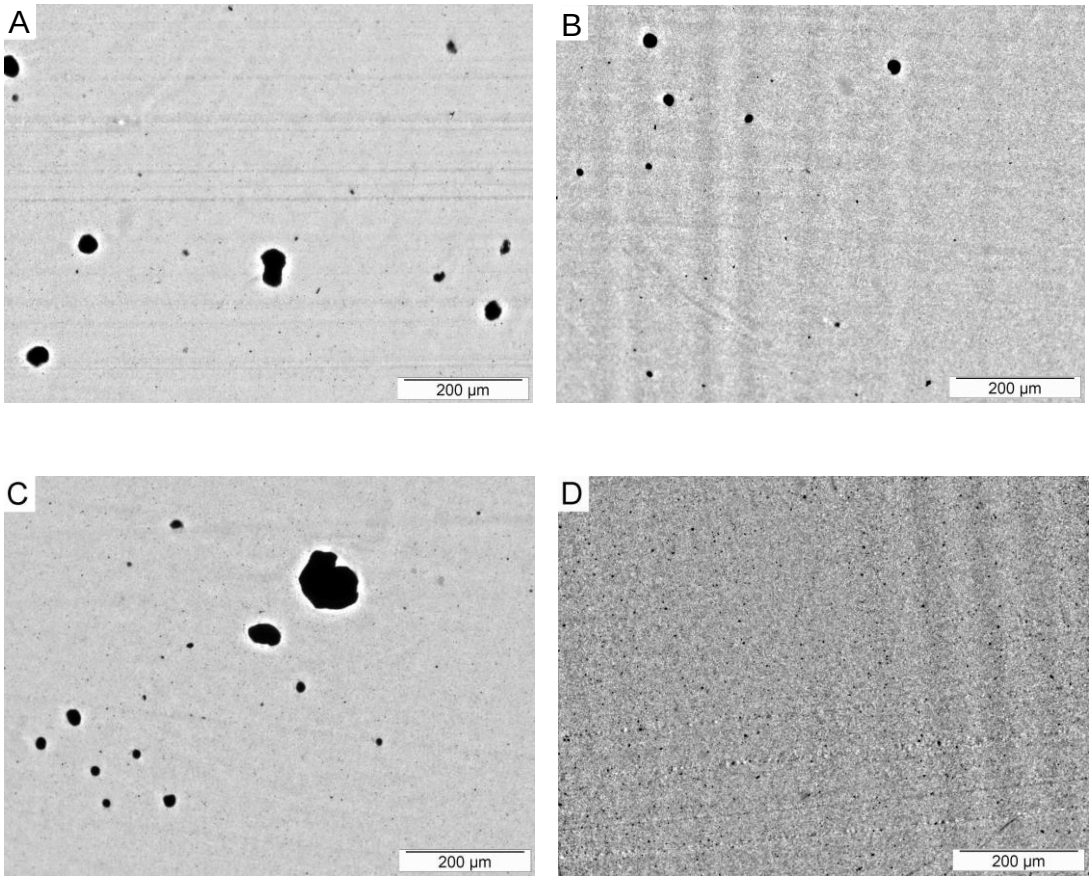

Figure 3

A 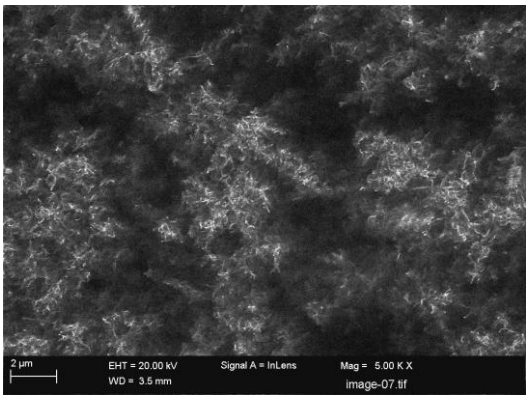

B 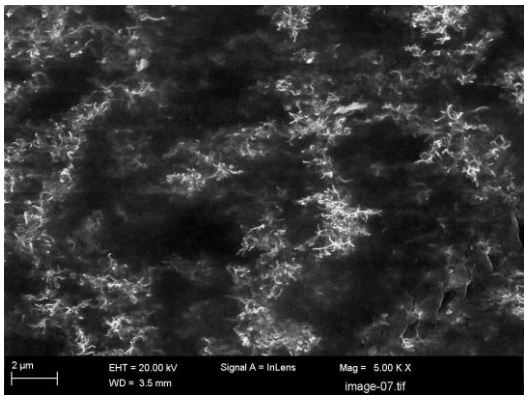

C 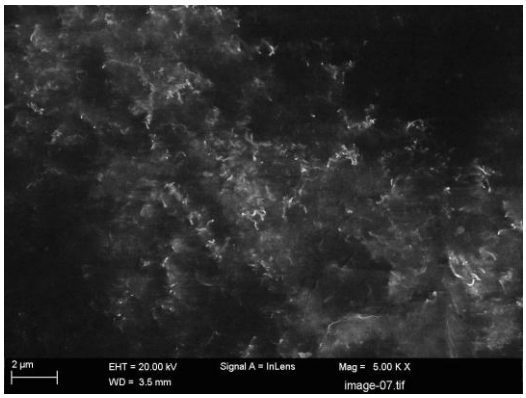

Figure 4.

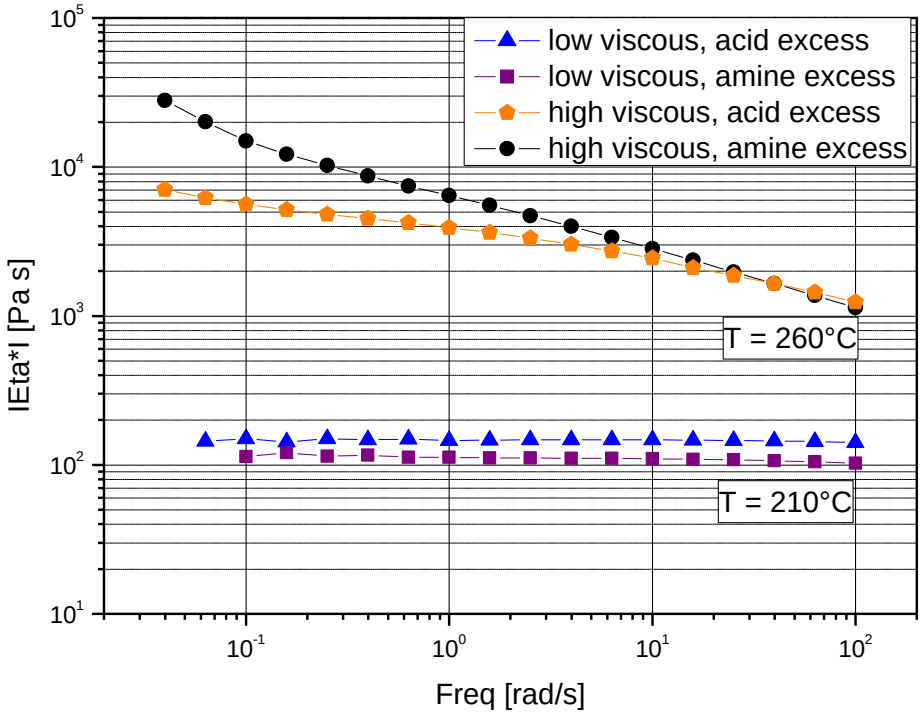

Figure 5.

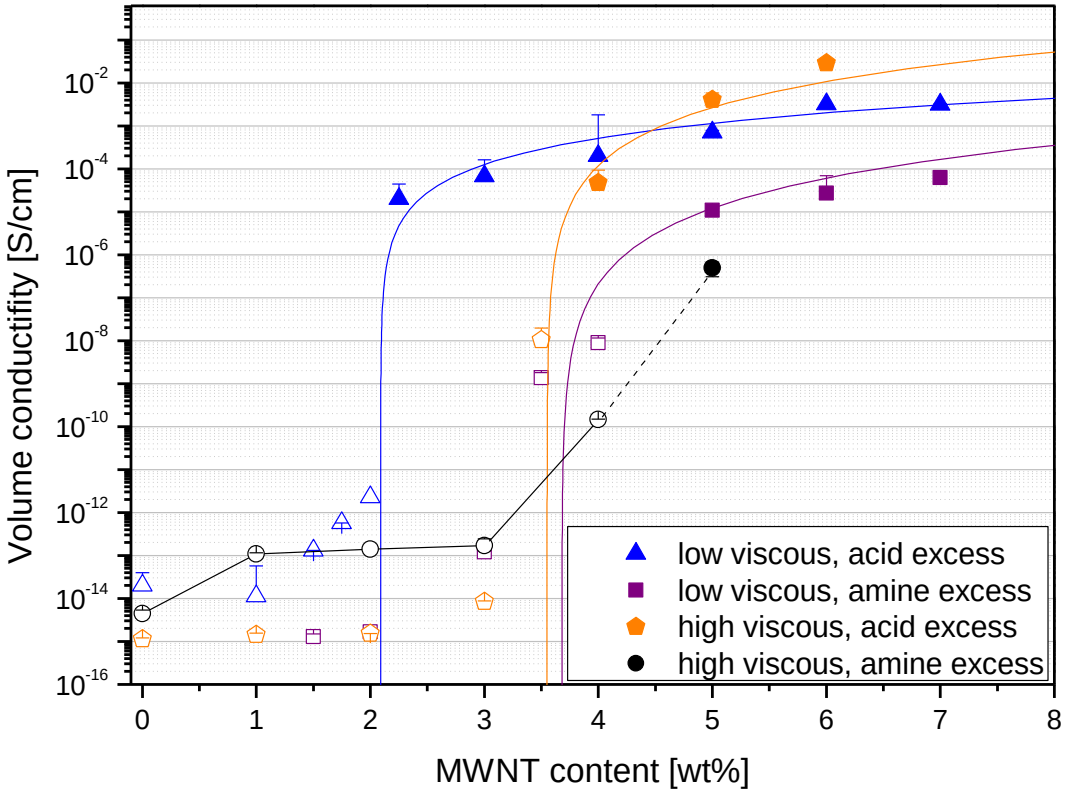

Figure 6.

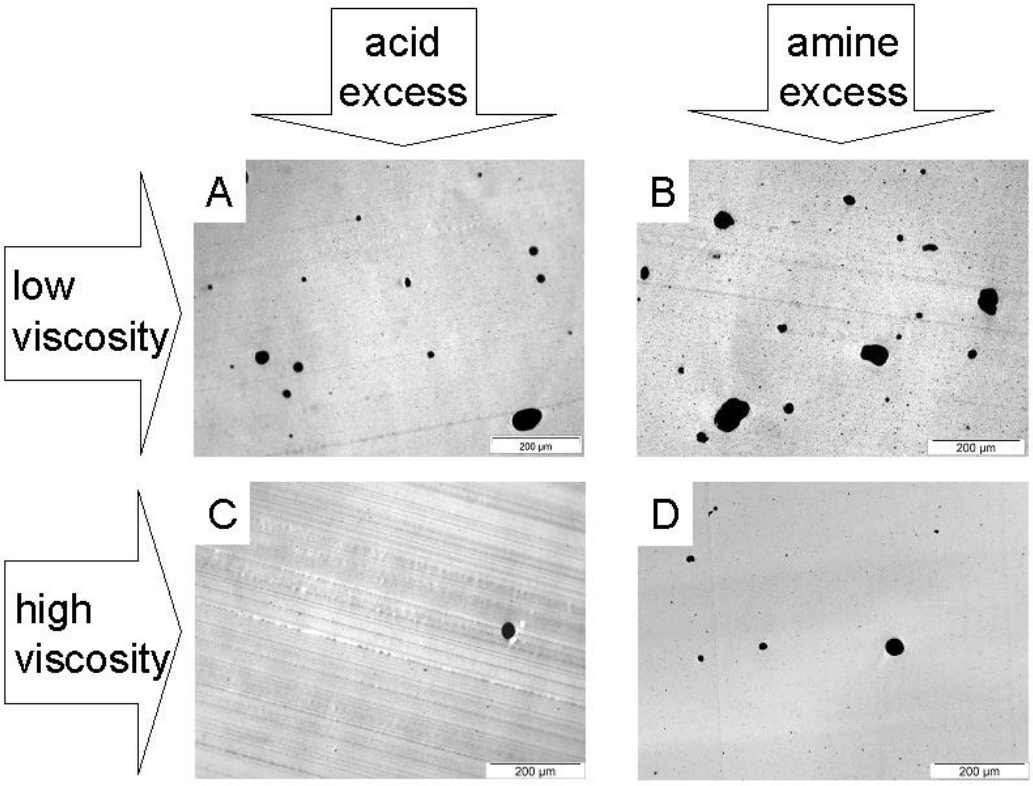

Figure 7.

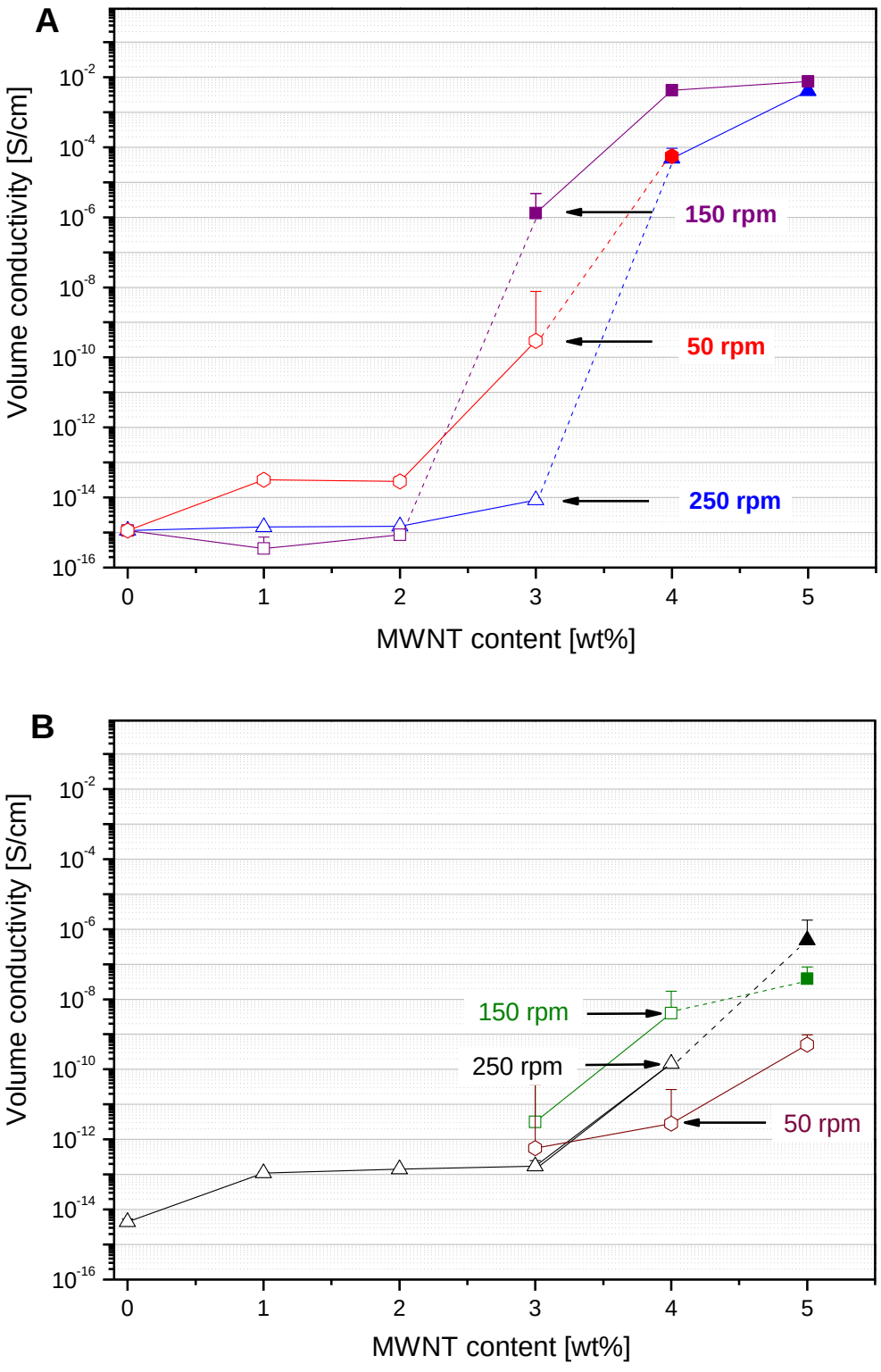
A
Volume conductivity [S/cm]
10-2
10-4
10-6
10-8
10-10
10-12
10-14
10-16
0
1
2
3
4
5
MWNT content [wt%]
150 rpm
50 rpm
250 rpm
B
Volume conductivity [S/cm]
MWNT content [wt%]
150 rpm
250 rpm
50 rpm

Figure 8

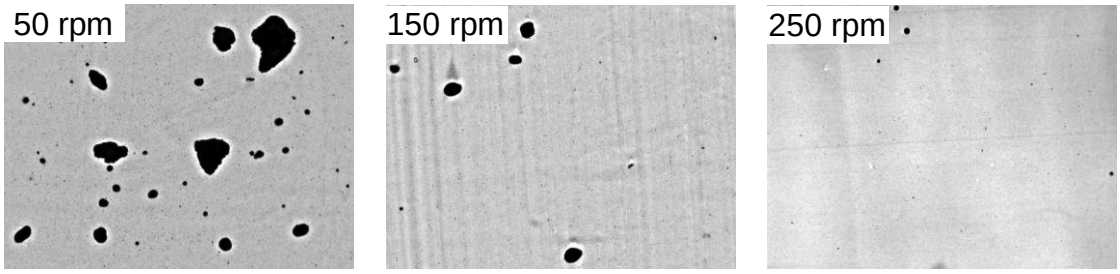

Figure 9